Electronic Supplementary Material (ESI) for Journal of Materials Chemistry A.


# Construction of self-supported leaf thorn-like nickel-cobalt bimetal phosphides as an efficient bifunctional electrocatalysts for urea electrolysis

Linna Sha, Jinling Yin, Ke Ye*, Gang Wang, Kai Zhu, Kui Cheng, Jun Yan, Guiling Wang, Dianxue Cao*

Key Laboratory of Superlight Materials and Surface Technology of Ministry of Education, College of Materials Science and Chemical Engineering, Harbin Engineering University, Harbin, 150001, PR China

*Corresponding authors.
E-mail addresses: yeke@hrbeu.edu.cn (K. Ye); caodianxue@hrbeu.edu.cn (D. Cao)

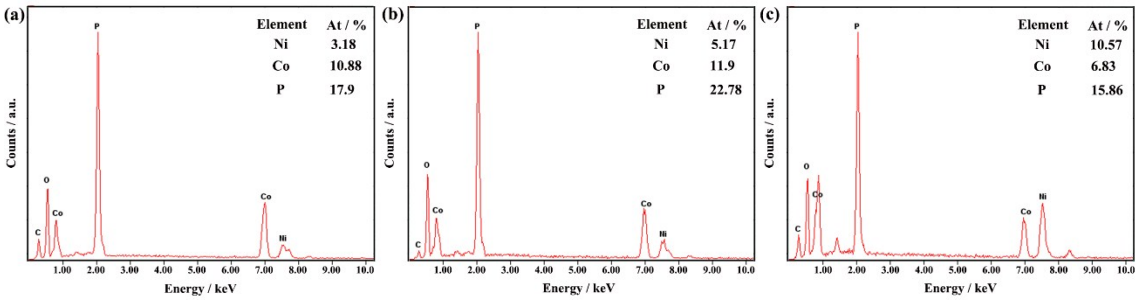


**Figure S1.** EDS spectra of (a) $Ni_{0.22}Co_{0.78}P$/CC, (b) $Ni_{0.31}Co_{0.69}P$/CC and (c) $Ni_{0.61}Co_{0.39}P$/CC.

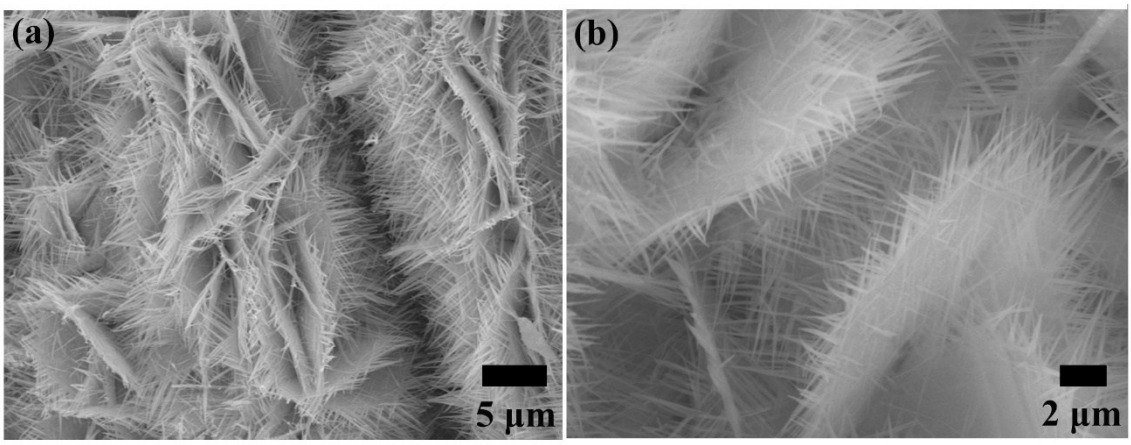


**Figure S2.** (a) Low-magnification and (b) high-magnification SEM images of the NiCo-OH/CC precursor.

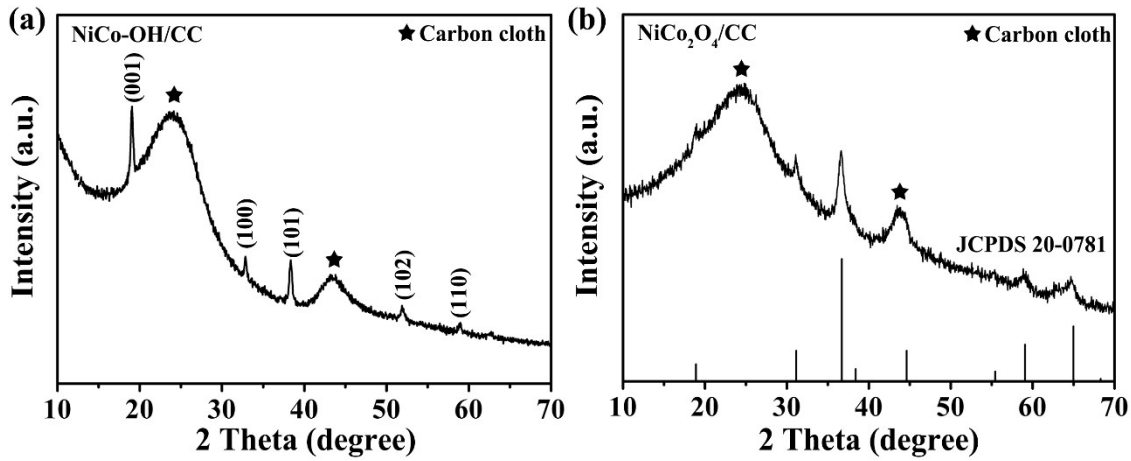


**Figure S3.** XRD patterns of the (a) NiCo-OH/CC precursor and (b) $NiCo_2O_4$/CC.

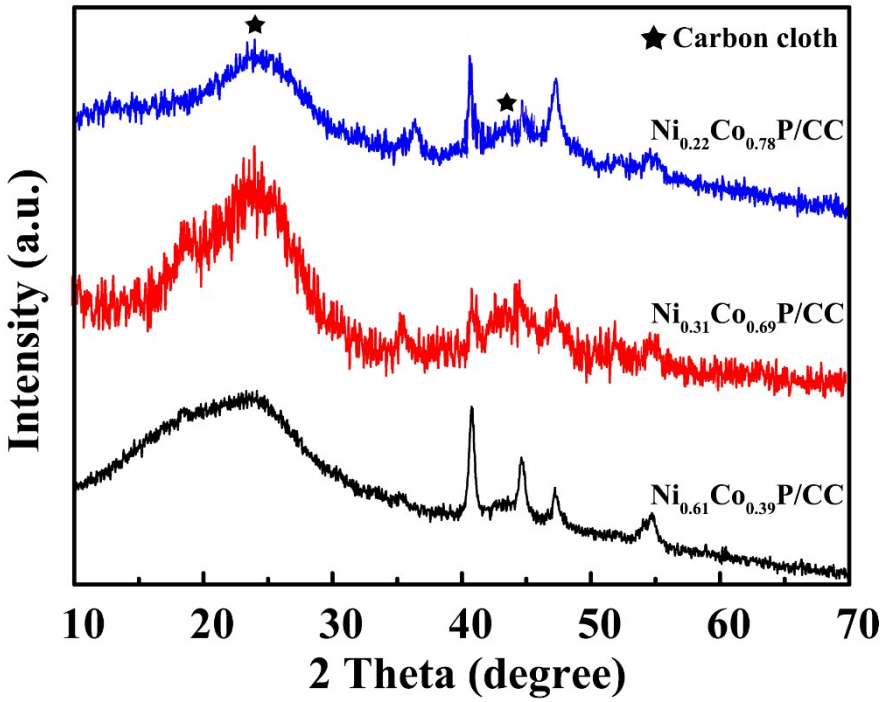


**Figure S4.** XRD patterns of the as-prepared $Ni_{1-x}Co_xP$/CC samples: $Ni_{0.22}Co_{0.78}P$/CC, $Ni_{0.31}Co_{0.69}P$/CC and $Ni_{0.61}Co_{0.39}P$/CC.

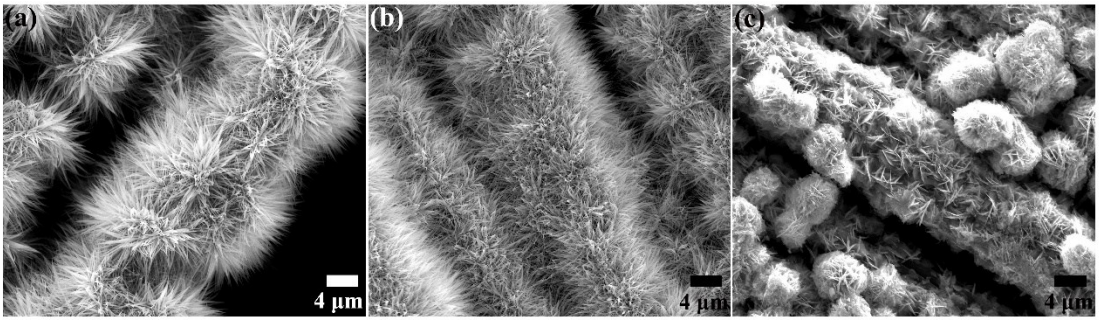


**Figure S5.** SEM images of (a) $Ni_{0.22}Co_{0.78}P$/CC, (b) $Ni_{0.31}Co_{0.69}P$/CC and (c) $Ni_{0.61}Co_{0.39}P$/CC.

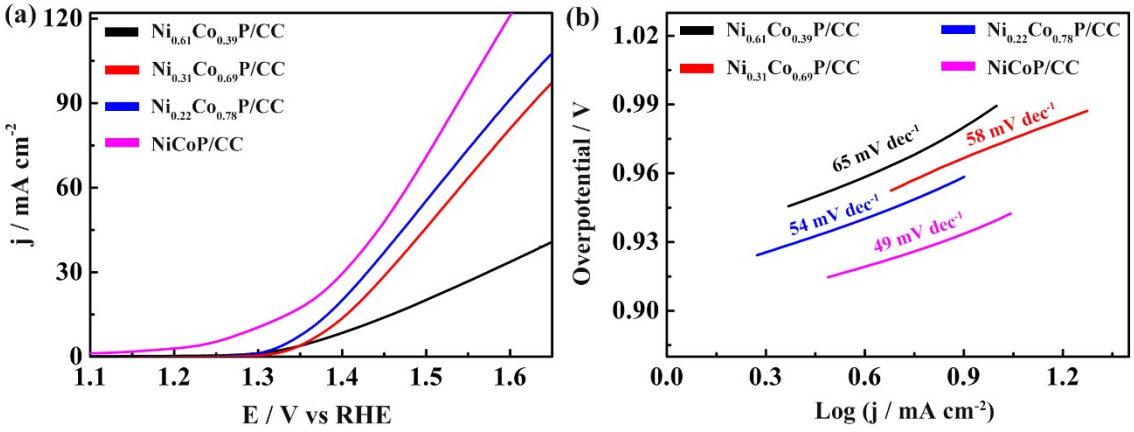


**Figure S6.** (a) LSV curves and (b) Tafel plots of the $Ni_{0.61}Co_{0.39}P$/CC, $Ni_{0.31}Co_{0.69}P$/CC, $Ni_{0.22}Co_{0.78}P$/CC and NiCoP/CC catalysts for UOR in 1 M KOH and 0.5 M urea.

Figure S6a shows the LSV polarization curves of all bimetallic phosphide electrodes with different Ni/Co ratios in 1.0 M KOH and 0.5 M urea. It is clearly noted that the UOR activity decreases with the decrease of the Co doping concentration. Specifically, NiCoP/CC electrode exhibited superior UOR activity with a lowest potential of 1.30 V at the current density of 10 mA $cm^{-2}$, which is much smaller than those of $Ni_{0.22}Co_{0.78}P$/CC (1.33 V), $Ni_{0.31}Co_{0.69}P$/CC (1.36 V) and $Ni_{0.61}Co_{0.39}P$/CC (1.38 V) electrodes. Meanwhile, the smaller Tafel slope of NiCoP/CC (49 mV $dec^{-1}$)

indicates its faster UOR kinetics than other samples (Figure S6b).

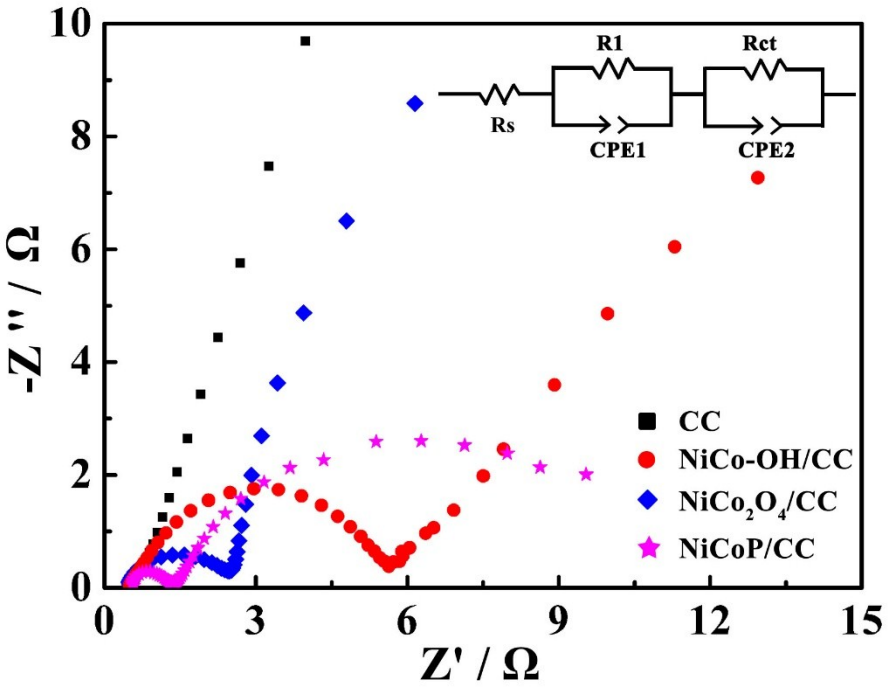


**Figure S7.** Nyquist plots of NiCoP/CC, $NiCo_2O_4$/CC, NiCo-OH/CC and bare CC catalysts for UOR process at 1.32 V vs. RHE.

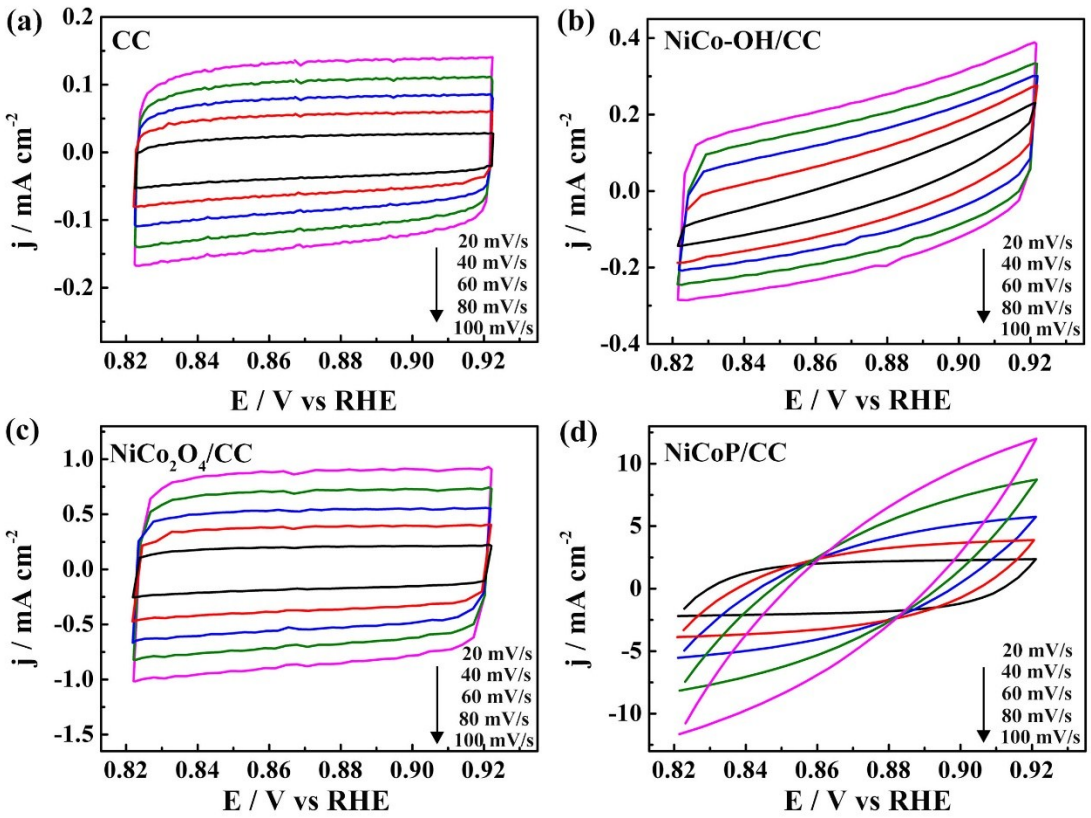


**Figure S8.** Cyclic voltammetry curves for (a) CC, (b) NiCo-OH/CC, (c) $NiCo_2O_4$/CC and (d) NiCoP/CC electrodes in the region of 0.82-0.92 V vs. RHE with different scanning rates upon UOR catalysis.

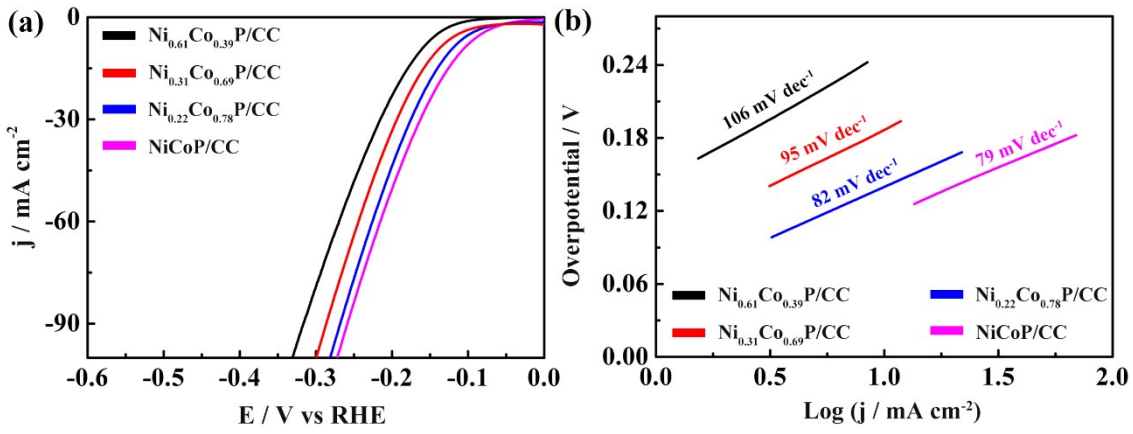


**Figure S9.** (a) LSV curves and (b) Tafel plots of the $Ni_{0.61}Co_{0.39}P/CC$, $Ni_{0.31}Co_{0.69}P/CC$, $Ni_{0.22}Co_{0.78}P/CC$ and NiCoP/CC catalysts for HER in 1 M KOH solution.

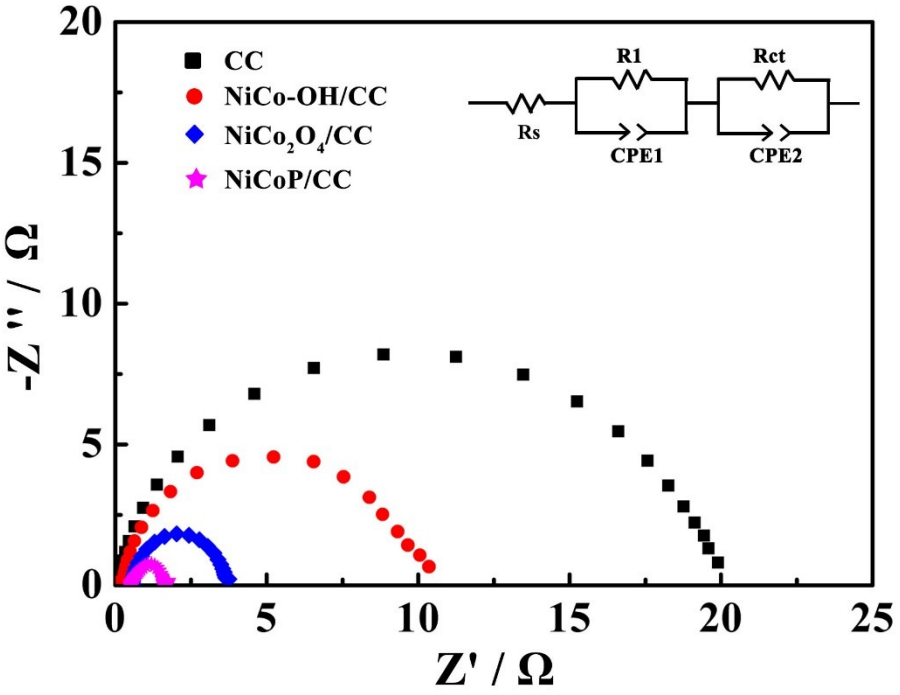


**Figure S10.** Nyquist plots of NiCoP/CC, $NiCo_2O_4$/CC, NiCo-OH/CC and bare CC catalysts at an overpotential of 300 mV toward HER.

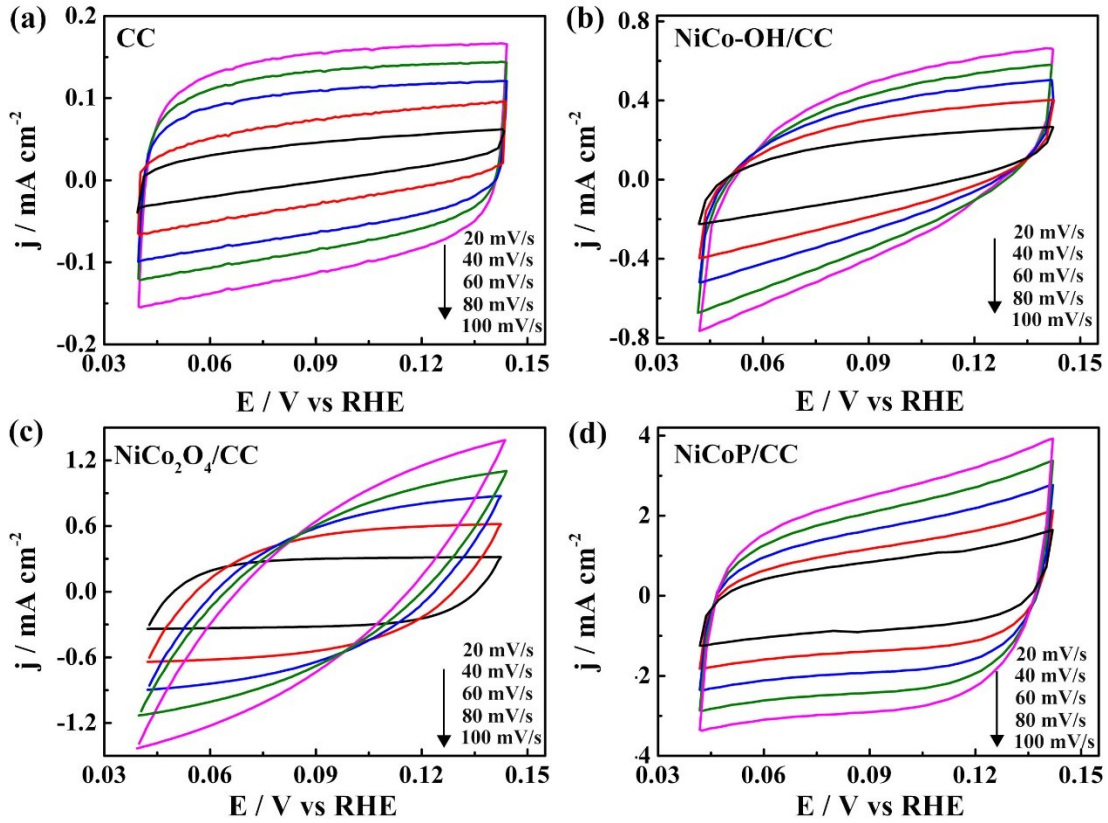


**Figure S11.** Cyclic voltammetry curves for (a) CC, (b) NiCo-OH/CC, (c) $NiCo_2O_4$/CC and (d) NiCoP/CC electrodes in the region of 0.04-0.14 V vs. RHE with different scanning rates upon HER catalysis.

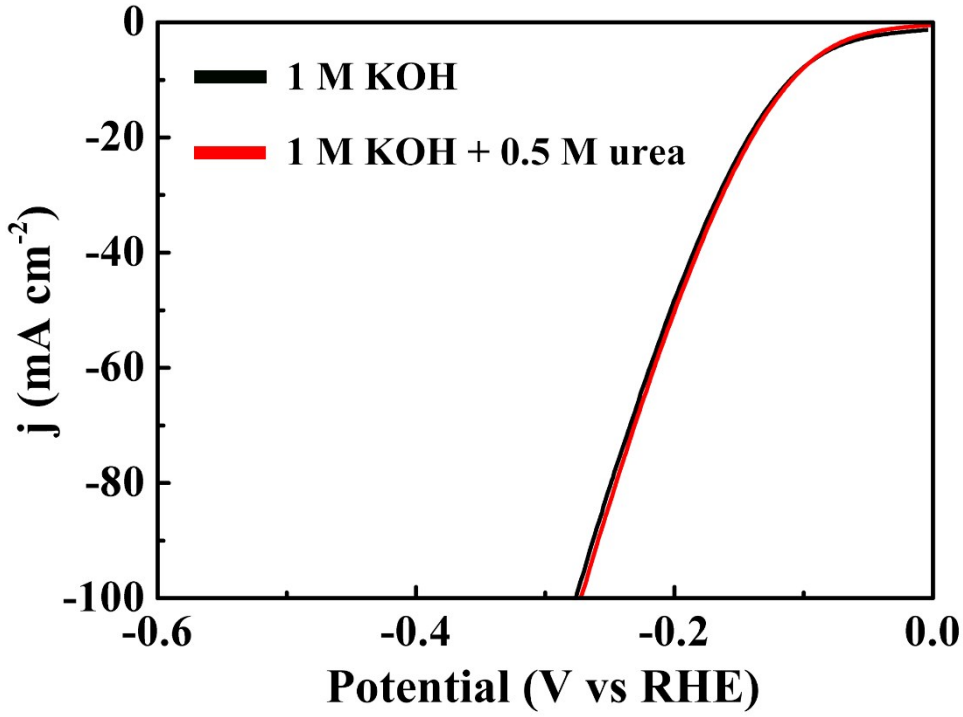


**Figure S12.** Polarization curves of NiCoP/CC in 1.0 M KOH with and without 0.5 M urea at a scan rate of 2 mV $s^{-1}$ for HER.

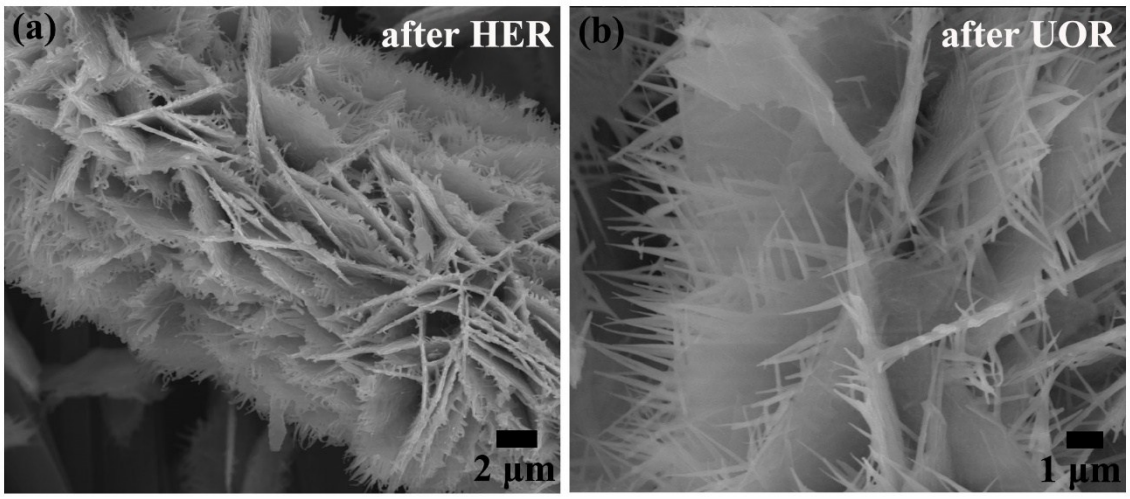


**Figure S13.** SEM images of NiCoP/CC after (a) HER and (b) UOR stability test.

**Table S1.** Comparison of the UOR performance of NiCoP/CC catalyst with other reported UOR catalysts.

| Catalysts | Urea concentrate (M) | j (mA $cm^{-2}$) | Voltage (V vs RHE) | References |
|---|---|---|---|---|
| $Ni(OH)_2$ | 0.33 | 10 | 1.42 | 1 |
| $Fe_{11.1\%}$-$Ni_3S_2$/Ni | 0.33 | 10 | 1.35 | 2 |
| NF/NiMoO | 0.5 | 10 | 1.37 | 3 |
| $Ni_3N$/CC | 0.33 | 10 | 1.35 | 4 |
| $Ni(OH)_2$-grephene | 0.33 | 10 | 1.43 | 5 |
| $MnO_2$/$MnCo_2O_4$/Ni | 0.5 | 10 | 1.33 | 6 |
| $Ni_2P$/CFC | 0.33 | 10 | 1.34 | 7 |
| NF/$MnO_2$ | 0.5 | 10 | 1.33 | 8 |
| $NiCo_2S_4$/CC | 0.33 | 10 | 1.35 | 9 |
| $Ni_3Se_4$ | 0.5 | 10 | 1.38 | 10 |
| **NiCoP/CC** | **0.5** | **10** | **1.30** | **This work** |

**Table S2.** Comparison of the HER performance of NiCoP/CC with other reported non-precious electrocatalysts in 1M KOH electrolyte.

| Catalysts | j ($mA\ cm^{-2}$) | $\eta_j$ (mV) | Tafel slope ($mV\ dec^{-1}$) | References |
|---|---|---|---|---|
| NiFeS/Ni | 10 | 180 | 53 | 11 |
| MoP | 10 | 52 | 40 | 12 |
| $NiCo_2S_4$/Ni | 10 | 210 | 58.9 | 13 |
| $FePo_4$ | 10 | 123 | 104.5 | 14 |
| $Ni(OH)_2/Ni_3S_2$ | 20 | 211 | 129 | 15 |
| CC/CoP | 10 | 110 | 129 | 16 |
| $Ni_3S_2$ | 10 | 60.8 | 67.5 | 17 |
| NiMoP | 10 | 135 | 137.5 | 18 |
| $Ni_{12}P_5$ | 10 | 107 | 63 | 19 |
| $MoS_2$-$Ni_3S_2$/NF | 10 | 110 | 83 | 20 |
| NiSe/NF | 10 | 96 | 120 | 21 |
| NiCoP/CC | **10** | **107** | **79** | **This work** |

**References**

[1] X. Zhu, X. Dou, J. Dai, X. An, Y. Guo, L. Zhang, S. Tao, J. Zhao, W. Chu, X. C. Zeng, C. Wu and Y. Xie, *Angew. Chem. Int. Ed.*, 2016, **55**, 12465-12469.

[2] W. X. Zhu, Z. H. Yue, W. T. Zhang, N. Hu, Z. T. Luo, M. R. Ren, Z. J. Xu, Z. Y. Wei, Y. R. Suo and J. L. Wang, *J. Mater. Chem. A*, 2018, **6**, 4346-4353.

[3] Z. Y. Yu, C. C. Lang, M. R. Gao, Y. Chen, Q. Q. Fu, Y. Duan and S. H. Yu, *Energ. Environ. Sci*., 2018, **11**, 1890-1897.

[4] Q. Liu, L. S. Xie, F. L. Qu, Z. Liu, G. Du, M. A. Abdullah and X. P. Sun, *Inorg. Chem. Front*., 2017, **4**, 1120-1124.

[5] D. Wang, W. Yan, S. H. Vijapur and G. G. Botte, *Electrochem. Acta*, 2013, **89**, 732-736.

[6] C. L. Xiao, S. N. Li, X. Y. Zhang and D. R. MacFarlane, *J. Mater. Chem. A*, 2017, **5**, 7825-7832.

[7] X. Zhang, Y. Y. Liu, Q. Z. Xiong, G. Q. Liu, C. J. Zhao, G. Z. Wang, Y. X. Zhang, H. M. Zhang and H. J. Zhao, *Electrochim. Acta*, 2017, **254**, 44-49.

[8] S. Chen, J. Duan, A. Vasileff and S. Z. Qiao, *Angew. Chem. Int. Ed*., 2016, **55**, 3804-3808.

[9] W. X. Zhu, M. R. Ren, N. Hu, W. T. Zhang, Z. T. Luo, R. Wang, J. Wang, L. J. Huang, Y. R. Suo and J. L. Wang, *ACS Sustainable Chem. Eng*., 2018, **6**, 5011-5020.

[10] J. Y. Zhang, X. N. Tian, T. He, S. Zaman, M. Miao, Y. Yan, K. Qi, Z. H. Dong, H. F. Liu and B. Xia, *J. Mater. Chem. A*, 2018, **6**, 15653-15658.

[11] P. Ganesan, A. Sivanantham and S. Shanmugam, *J. Mater. Chem. A*, 2016, **4**, 16394-16402.

[12] X. Zhang, F. Zhou, W. Y. Pan, Y. Y. Liang, and R. H. Wang, *Adv. Funct. Mater*., **28**, 1804600.

[13] A. Sivanantham, P. Ganesan and S. Shanmugam, *Adv. Funct. Mater.*, 2016, **26**, 4661-4672.

[14] L. Yang, Z. L. Guo, J. Huang, Y. N. Xi, R. J. Gao, G. Su, W. Wang, L. X. Cao, and B. H. Dong, *Adv. Mater*., 2017, **29**, 1704574.

[15] X. Q. Du, Z. Yang, Y. Li, Y. Q. Gong and M. Zhao, *J. Mater. Chem. A*, 2018, **6**, 6938-6946.

[16] J. Tian, Q. Liu, A. M. Asiri and X. Sun, *J. Am. Chem. Soc*., 2014, **136**, 7587-7590.

[17] C. Yang, M. Y. Gao, Q. B. Zhang, J. R. Zeng, X. T. Li and A. P. Abbott, *Nano Energy*, 2017, **36**, 85-94.

[18] H. Xu, J. J. Wei, K. Zhang, Y. Shiraishi, and Y. K. Du, *ACS Appl. Mater. Interfaces*, 2018, **10**, 29647-29655.

[19] Z. P. Huang, Z. B. Chen, Z. Z. Chen, C. C. Lv, H. Meng, and C. Zhang, *ACS Nano*, 2014, **8**, 8121-8129.

[20] J. Zhang, T. Wang, D. Pohl, B. Rellinghaus, R. Dong, S. Liu, X. Zhuang and X. Feng, *Angew. Chem. Int. Ed*., 2016, **55**, 6702-6707.

[21] C. Tang, N. Y. Cheng, Z. H. Pu, W. Xing, and X. P. Sun, *Angew. Chem. Int. Ed*., 2015, **54**, 9351-9355.